

Corrosion behaviour of die-cast AZ91D magnesium alloys in sodium sulphate solutions with different pH values

TIAN Yun¹, YANG Li-jing¹, LI Yan-fang¹, WEI Ying-hui¹, HOU Li-feng¹, LI Yong-gang¹, Ri-Ichi MURAKAMI²

1. College of Materials Science and Engineering,

Taiyuan University of Technology, Taiyuan 030024, China;

2. Department of Mechanical Engineering, University of Tokushima, Tokushima 770-8506, Japan

Received 25 September 2010; accepted 25 December 2010

Abstract: The corrosion behaviours of die-cast AZ91D magnesium alloys were investigated in 0.1 mol/L sodium sulphate (Na_2SO_4) solutions with different pH values. The corrosion rates, morphologies, and compositions of the corrosion products were studied by means of scanning electron microscopy (SEM), Fourier transform infrared spectroscopy (FTIR), and X-ray diffractometry (XRD). The results indicate that the order of corrosion rates in Na_2SO_4 solutions with various pH values is $\text{pH } 2 > \text{pH } 4 > \text{pH } 7 > \text{pH } 9 > \text{pH } 12$. The corrosion rates in acidic solutions are higher than those in alkaline solutions, and the corrosion products are mainly magnesium hydroxide ($\text{Mg}(\text{OH})_2$) and hydrated sulphate pickeringite ($\text{MgAl}_2(\text{SO}_4)_4 \cdot 22\text{H}_2\text{O}$). The results also indicate that the solution pH can influence the corrosion rate and morphology of corrosion products. Chloride ions and sulphate ions have different pitting initiation time.

Key words: magnesium alloy; corrosion; sodium sulphate; pH value

1 Introduction

Magnesium alloys have received extensive recognition as a new type of environmentally friendly material because of their excellent physical properties, including low density, high specific strength, and good electromagnetic shielding[1–2]. These alloys have wide applications and exploitation prospects. However, the use of Mg alloys remains limited because of their susceptibility to corrosion. Therefore, studies on the corrosion behaviour of Mg alloys in active media, especially those containing aggressive ions, are crucial to understanding its corrosion mechanisms, which would determine an effective way to protect Mg alloys.

A consensus appears to have been reached regarding the corrosion mechanism underlying the aggressive behaviour of sodium chloride against Mg[3–5]. However, the corrosion process of Mg alloys in solutions containing SO_4^{2-} remains ambiguous. With more and more Mg alloy applications exposed to the

atmospheric environment, the effect of acid rain on Mg alloys has become the focus of various studies. Because SO_4^{2-} plays an important role in the formation of acid rain, studying the effects of SO_4^{2-} in solution is a suitable experimental design. YANG et al[6] studied the corrosion behaviours of die-cast AZ91D in NaCl, Na_2SO_4 , and MgSO_4 solutions. When the immersion time was less than 48 h, pitting occurred on the specimen surfaces immersed in NaCl solution, whereas general corrosion was apparent in those immersed in SO_4^{2-} solutions. Characteristic models of corrosion behaviour in acid, alkaline, and neutral solutions and a double electronic layer model were established by ZHANG[7], and the corrosion behaviours of ingot AZ91D in Na_2SO_4 solutions with different pH values were studied. CHEN et al[8–9] studied the corrosion behaviours of ingot AZ91D in various 0.1 mol/L Na_2SO_4 solutions by alternate current (AC) impedance spectroscopy. When the immersion time was less than 181 h, general corrosion occurred on the specimen surface. With prolonging immersion time, pitting began to appear on

Foundation item: Project (51044007) supported by the National Natural Science Foundation of China; Project (08121018) supported by the Science and Technology Project of Taiyuan City, China; Project (20091402110010) supported by the Doctoral Found of Ministry of Education of China; Project (2008029) supported by the Shanxi Province Foundation for Returned Scholars, China; Project (20093007) supported by the Young Subject-Leader Foundation and the Innovative Project for Outstanding Post-graduate of Shanxi Province, China

Corresponding author: WEI Ying-hui; Tel/Fax: +86-351-6018683; E-mail: yhwei@public.ty.sx.cn

DOI: 10.1016/S1003-6326(11)60801-7

the surface, and the corrosion rate relied on the concentration of products.

Although some studies have focused on the corrosion behaviour of an AZ91D alloy in ingot specimens immersed in Na₂SO₄ solutions, few reports referred to the corrosion behaviour of die-cast AZ91D alloys in Na₂SO₄ solutions with different pH values. To date, an increasing number of die-cast Mg alloy components have been used daily. Therefore, a study of the corrosion mechanism of die-cast AZ91D in Na₂SO₄ solution is necessary. In this work, the effects of pH value and SO₄²⁻ ions on the corrosion behaviour of die-cast AZ91D were systematically studied.

2 Experimental

2.1 Materials

The specimens were made of die-cast AZ91D Mg alloy. During the die-casting process, the die temperature was controlled at 280–300 °C, and the molten metal temperature was held at (630±20)° C. The cycle time for the product was 38–45 s, and the cast pressure was 40 MPa. The component was 1 mm in nominal thickness. The chemical composition of the sample is shown in Table 1.

2.2 Immersion test

Ninety specimens with dimensions of 15 mm × 15 mm × 1 mm, were prepared for the immersion tests at room temperature. Prior to testing, the specimens were numbered and polished with SiC papers with up to 1200 grit to meet the requirements of the corrosion tests. The specimens were then cleaned with acetone and dried. The original mass and surface area of the specimens were measured by a BS110S electronic balance and a slide caliper, respectively. The corrosion media were 0.1 mol/L Na₂SO₄ solutions, maintained in open air at about 20 °C with pH values of 2, 4, 7, 9 and 12. The specimens were immersed in Na₂SO₄ solutions with various pH values for 4, 48, 96, 180, 330 and 480 h. The specimens were retrieved at pre-determined time points and immersed in boiling chromic acid solution (200 g/L CrO₃ + 10 g/L AgNO₃) for 3–5 min to remove the corrosion products. Specimens were then cleaned with de-ionized water and alcohol, and dried. After the removal of corrosion products, the specimens were again weighed to obtain their final mass. The corrosion

rate of the specimen was calculated as follows:

$$v = (m_0 - m_1) / (St) \quad (1)$$

where m_0 is the original mass of the specimen; m_1 is the final mass of the specimen without corrosion products; S is the surface area; and t is the immersion time.

2.3 Analysis and characterization methods

The surface and cross-sectional morphologies of the specimens after the immersion tests were observed with scanning electron microscope (SEM). The corrosion products were analyzed by energy dispersive X-ray spectroscopy (EDS) and X-ray diffraction spectroscopy (XRD). Then, the specimen surface was scraped, and the samples were analyzed via Fourier transform infrared spectroscopy (FTIR). The specimens without corrosion were tested for surface roughness using a TR240 portable surface roughness tester to measure pitting depth.

Potentiodynamic polarization curves were measured using pre-treated magnesium specimens immersed in corrosion solutions at room temperature (20 °C). A three-electrode cell was employed in this test. The working electrode was the test material, the counter electrode was the platinum sheet, and the reference electrode was the saturated calomel electrode (SCE). The working electrode was embedded in an epoxy resin to provide insulation, leaving a surface area of 1.0 cm² in contact with the electrolyte. The potential was scanned at a rate of 1 mV/s using a PGSTAT30 electrochemical workstation.

3 Results

3.1 Corrosion rate and mass loss

The relationships between mass losses and immersion time after the specimens were immersed in 0.1 mol/L Na₂SO₄ solutions with various pH values are shown in Fig.1. The mass losses of the specimens increased gradually as the immersion time increased. This indicates that the specimens are constantly corroded. The mass losses in different solutions decreased with increasing pH value. In acidic and neutral solutions, mass loss rose sharply when the immersion time exceeded 180 h. Mass loss increased faster when pH value was lower. In alkaline solutions, however, the mass loss increased slowly and finally remained constant. The

Table 1 Chemical composition of specimens studied (mass fraction, %)

Sample	Al	Zn	Mn	Si	Cu	Ni	Fe	Be	Mg
Experimental	8.89	0.67	0.211	0.0336	0.0045	<0.000 50	0.002 6	0.000 09	Bal.
Standard	8.5–9.5	0.45–0.90	0.17–0.40	0.08(max)	0.025(max)	0.001(max)	0.004(max)	(5–15)×10 ⁻⁶	Bal.

corrosion rates of all specimens declined with prolonging corrosion time (Fig.2). The corrosion rate of the specimen in solution with pH 2 was the highest among all solutions, and it decreased sharply until the immersion time reached 48 h. In the alkaline solutions, the decline in the corrosion rate was relatively slow. The corrosion rates of the specimens in solutions with pH 9 and 12 were nearly the same.

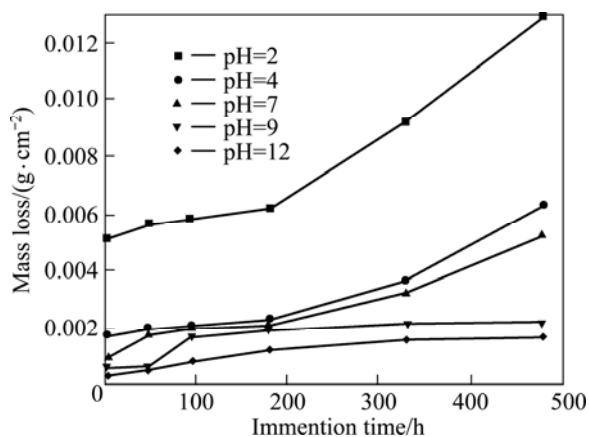


Fig.1 Mass loss for die-cast AZ91D alloys immersed for 4, 48, 96, 180, 330 and 480 h, respectively, in 0.1 mol/L Na_2SO_4 solutions with various pH values

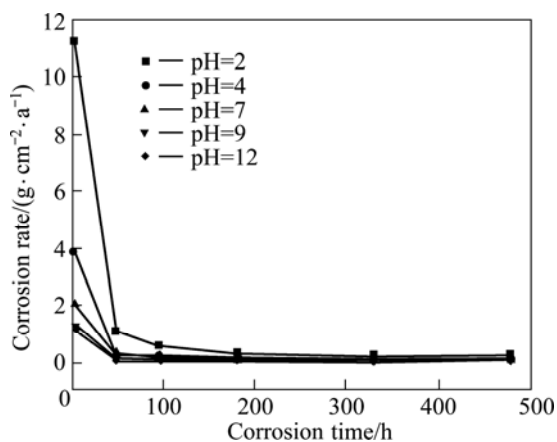


Fig.2 Corrosion rate for die-cast AZ91D alloys immersed for 4, 48, 96, 180, 330 and 480 h in 0.1 mol/L Na_2SO_4 solutions with various pH values

3.2 Corrosion product analysis

The X-ray diffraction (XRD) experiment was used to analyze the corrosion products of die-cast AZ91D Mg alloys immersed for 480 h in 0.1 mol/L Na_2SO_4 solutions with various pH values. Brucite [$\text{Mg}(\text{OH})_2$] was found to be the main corrosion product (Fig.3). In contrast to other solutions, the $\text{Mg}(\text{OH})_2$ peak was the most obvious in the solution with pH 2. In addition, the diffraction peak of $\text{Mg}(\text{OH})_2$ decreased gradually with increasing pH value.

FTIR spectroscopy was used to further identify the

constituents of the corrosion products. The specimens used for FTIR analysis were those immersed for 480 h in 0.1 mol/L Na_2SO_4 solutions with various pH values. $\text{MgAl}_2(\text{SO}_4)_4 \cdot 22\text{H}_2\text{O}$ was one of the corrosion products (Fig.4). Compared with the FTIR results, however, no $\text{MgAl}_2(\text{SO}_4)_4 \cdot 22\text{H}_2\text{O}$ peak was observed in the XRD patterns. This may mean that the amount of $\text{MgAl}_2(\text{SO}_4)_4 \cdot 22\text{H}_2\text{O}$ produced was very few. In solutions with pH 2 and 12, $\text{Mg}(\text{OH})_2$ appeared to be a corrosion product. However, $\text{Mg}(\text{OH})_2$ peaks could not be found in solutions with pH 4, 7, and 9. This may be due to the amount of by-products scraped from the surface of the specimens.

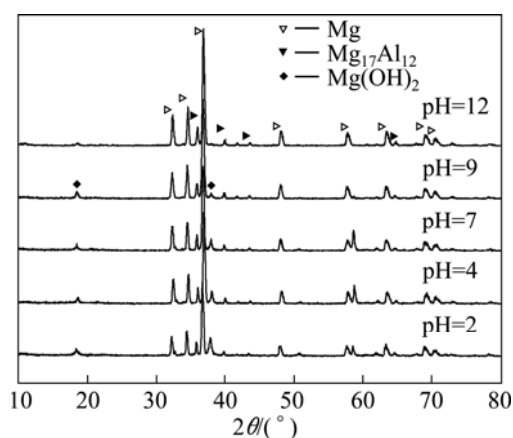


Fig.3 XRD patterns of corrosion products collected from five Na_2SO_4 solutions after die-cast AZ91D specimens immersed in 0.1 mol/L Na_2SO_4 solutions for 480 h with various pH values

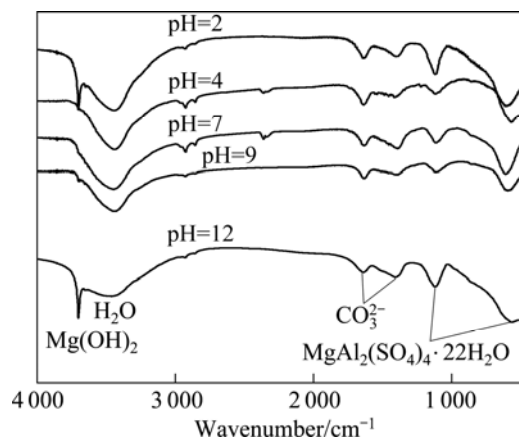


Fig.4 FTIR spectra of corrosion products scraped from specimens immersed in solutions with various pH values

3.3 Surface roughness

To measure the depth of the dents formed on the specimen surface, a surface roughness experiment was conducted after the corrosion products were removed. The relationships between surface roughness and immersion time after the specimens were immersed in

0.1 mol/L Na_2SO_4 solutions for 480 h with pH 2, 7, and 12 are shown in Fig.5. The roughness of the specimens immersed in the solution with pH 2 was much higher than that immersed in the two other solutions. When the corrosion time was prolonged, specimen surface roughness, as well as growth rate, in the solution with pH 2 increased consistently. In solutions with pH 7 and 12, the surface roughness of the die-cast Mg alloy AZ91D specimen initially increased and then decreased when the immersion time exceeded 96 h. Thus, the surface roughness of specimens that underwent corrosion tests decreases with increasing pH values.

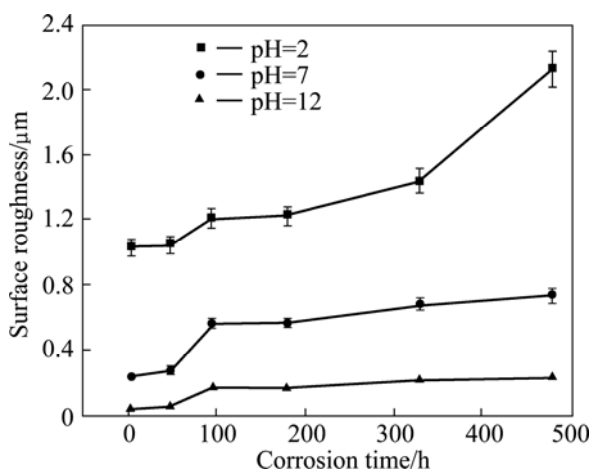


Fig.5 Surface roughness of specimens immersed in Na_2SO_4 solutions for 480 h with various pH values

3.4 Polarisation curves

The steady-state polarisation curves of specimens after immersion in Na_2SO_4 solutions are shown in Fig.6. The corrosion potentials of the specimens were -1.519 , -1.503 , -1.501 , -1.499 and -1.476 V in solutions with pH values of 2, 4, 7, 9, and 12, respectively. The order of corrosion potentials in various pH values is: $\text{pH } 2 < \text{pH } 4 < \text{pH } 7 < \text{pH } 9 < \text{pH } 12$.

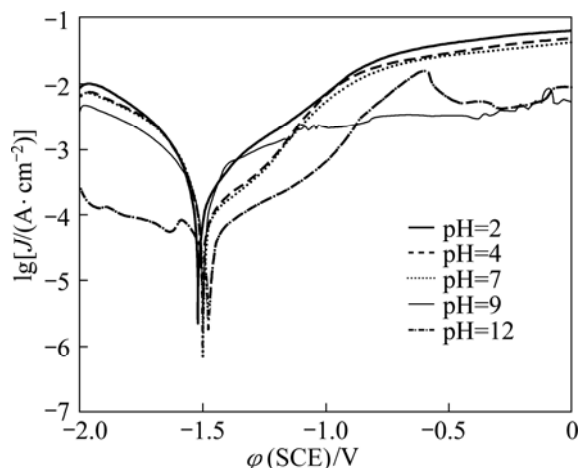


Fig.6 Polarisation curves of specimens in Na_2SO_4 solutions with various pH values

3.5 Corrosion morphologies

After specimens were immersed for 4, 48, 96, 180, 330, and 480 h, the specimen morphologies showed obvious differences. Visible corrosion became slighter as the pH value increased. In the solution with pH 2, the bubbles overflowed and broke away from the specimen surface. The metallic lustre of the specimen surface was also gradually lost, and corrosion became much more severe than in other specimens. As shown in Fig.7(a), general corrosion occurred on the specimen surface immersed for 48 h in the solution with pH 2. Well-distributed cracks were present on the surface. After 96 h immersion, the loss of the superficial layer from the surface of the specimen was very visible (Fig.7(b)). The corrosion product layer became

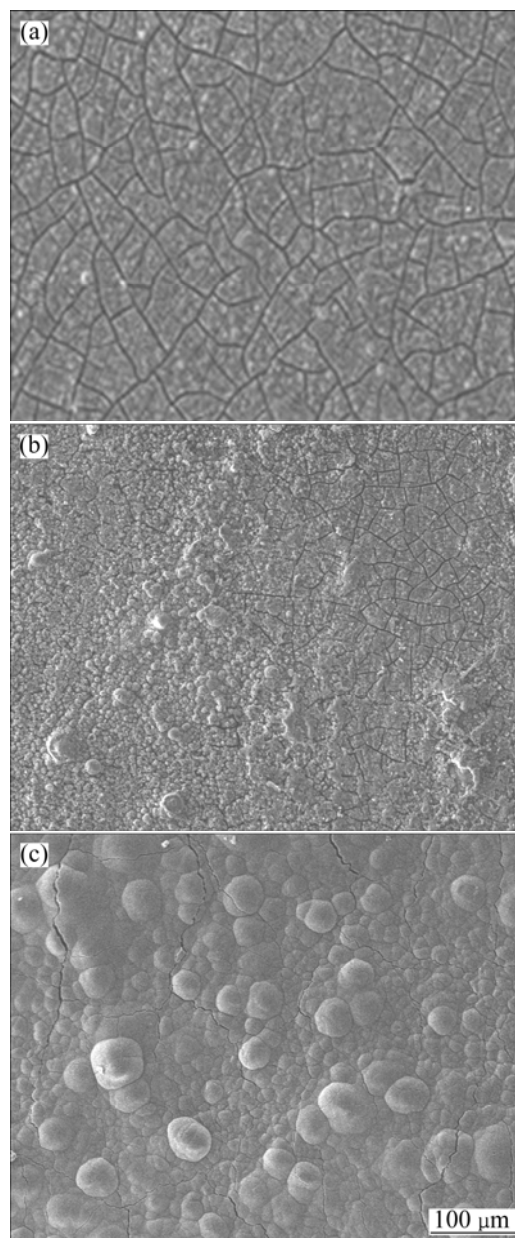


Fig.7 SEM morphologies of samples immersed in Na_2SO_4 solution with pH 2 for various time: (a) 48 h; (b) 96 h; (c) 480 h

thick and began to accumulate on the surface. When the immersion time exceeded 480 h, a hemisphere-like film formed on the surface. Compared with other immersion time, the hemisphere-like film was compact and relatively matte under this condition (Fig.7(c)).

After immersion in solutions with pH 4, 7 and 9, the specimen surfaces turned grey, and general corrosion occurred. The surface corrosion morphology of the specimen immersed for 96 h in the solution with pH 9 is shown in Fig.8(a). White reticulated lines formed on the surface. EDS results indicate that the white reticulated lines may be β -Mg₁₇Al₁₂. An acicular corrosion product formed on the surface of the specimens (Fig.8(b)). When the immersion time exceeded 480 h,

fine needle-like aggregates formed a film on the surface (Fig.8(c)). In the solution with pH 12, the specimen surfaces darkened, and little disruptions could be seen with the naked eye. EDS analysis indicates that the films consist of Mg, O, Al and S.

The morphologies of the specimen surfaces where the corrosion products were removed are shown in Fig.9. The specimens were immersed in different solutions for 480 h. Dents appeared in all the specimens, with deeper dents at lower pH values. There were some white netted phases around almost every dent. As shown in Fig.9(a), pitting occurred on the surface of the specimen in the solution with pH 2. The pitting dents were relatively deep, and penetration occurred at the bottom of the dents.

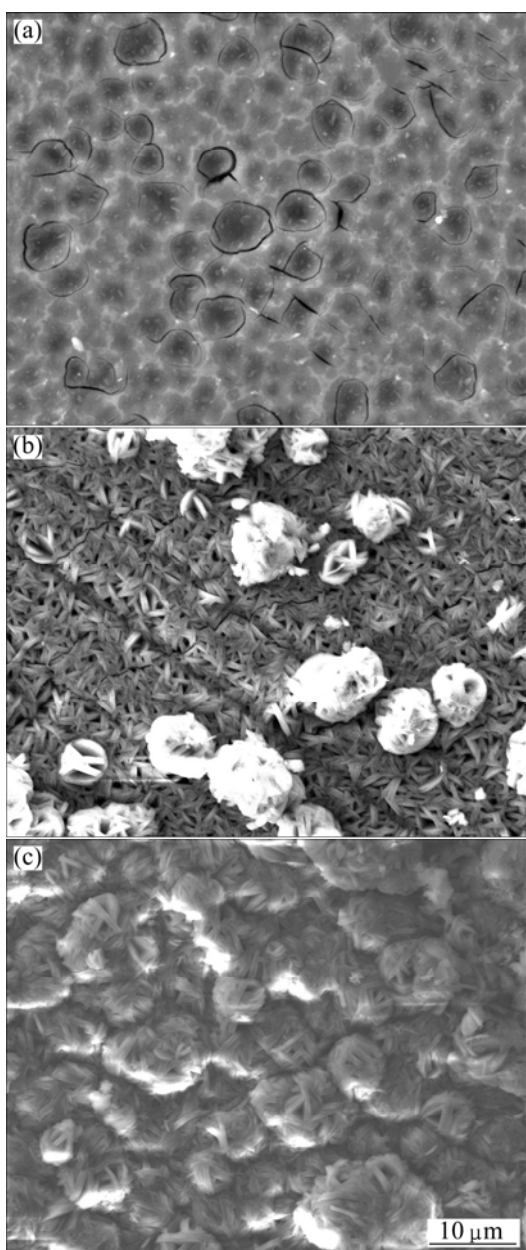


Fig.8 SEM images of specimens immersed in Na₂SO₄ solution with pH 9 for various time: (a) 96 h; (b) 330 h; (c) 480 h

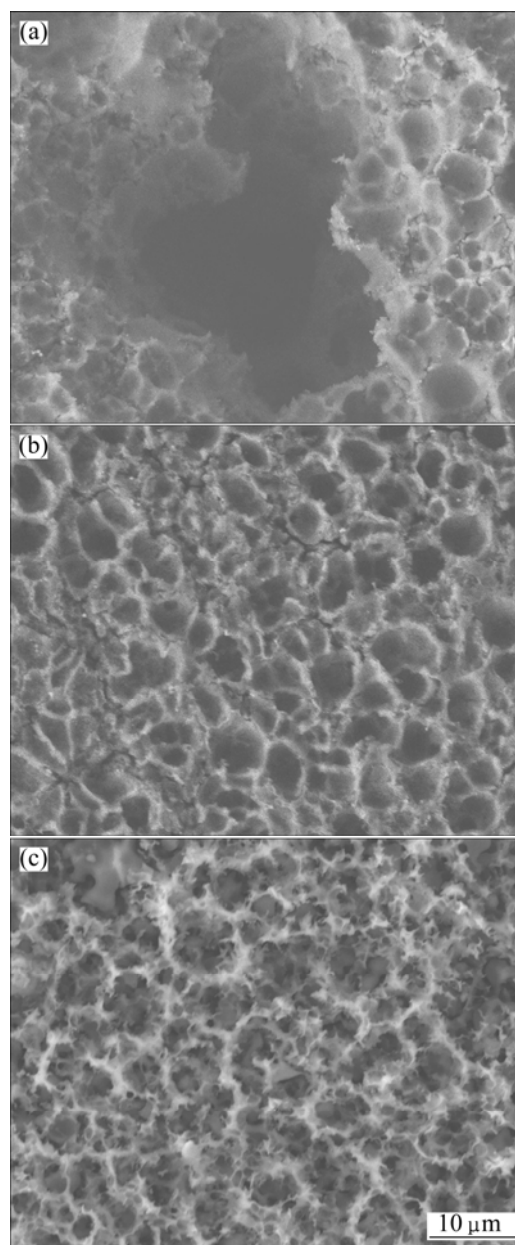


Fig.9 SEM images of surfaces after removing corrosion products: (a) pH 2; (b) pH 7; (c) pH 12

In the solutions with pH 4, dents were smaller than those formed with pH 2, and the dents grew and connected with each other. In solutions with pH 12, the specimen surfaces were uniformly distributed and homogeneous in size. EDS analysis showed that the aluminium content was higher in the white netted phases than that in the dents, indicating that the white phase was β -Mg₁₇Al₁₂.

The morphologies of the cross-sections of AZ91D alloy after immersion for 480 h at pH 2, 7 and 12 are shown in Fig.10. The corrosion product became thinner and thinner as the pH value increased. The corrosion product film of the specimen immersed in the solution

with pH 2 was 30 times thicker than that in the other two solutions. The surface of the specimen immersed in solution with pH 2 was rough due to the uneven distribution of corrosion products, causing some to fall off (Fig.10(a)). The product thickness differed significantly from one area of the specimen to another, and the thickest one of film was about 270 μm . Thin layers of corrosion products were visible on the matrix in solutions with pH 7 and 12 (Fig.10(b) and Fig.10(c)). For these solutions, films of corrosion products were uniform and their thicknesses were about 8 μm for the specimens immersed in solution with pH 7 and 7 μm for the specimens immersed in solution with pH 12.

4 Discussion

4.1 Effect of pH values on corrosion rates of AZ91D alloy

The anodic portions of the polarisation curves show that the corrosion current density, J_{corr} , of the solution with pH 2 is the highest, whereas the J_{corr} in the solution with pH 12 is the lowest. The J_{corr} of the die-cast AZ91D alloy in Na₂SO₄ solutions with pH 2, 7, and 12 were 0.0135, 0.00495, and 0.00185 mA/cm², respectively, as found by the Tafel extrapolation method. This indicates that the order of increasing corrosion rates in Na₂SO₄ solutions is: pH 2 > pH 7 > pH 12. Hence, the corrosion rate of the AZ91D alloy in acidic solutions was faster than that in neutral or alkaline solutions.

The relationships among electrode potential, corrosion rate and pH value of AZ91D Mg alloy are shown in Fig.11. The pH value had a great influence on both the electrode potential and the corrosion rate. When the pH value was less than 4, the corrosion rates declined with increasing pH value, while the electrode potentials presented the reverse reaction. When the pH values were from 4 to 9, the corrosion rates of the specimens showed a tendency to decrease slowly, and the electrode potentials were comparatively stable with a potential of -1.5 V. When the pH value was larger than 9, the trend of the corrosion rates changed more smoothly. When the pH value was less than 3, the balanced potential of hydrogen moved toward a positive direction[10] and corrosion was prone to becoming aggravated. Thus, in the solution with pH 2, the corrosion reaction proceeded rapidly at first, forming a corrosion product with the time prolonging. Thermodynamic and $\phi(\text{SCE})$ -pH diagrams predicted that Mg(OH)₂ will not be stable under such conditions. However, the dissolution kinetics for the reaction may be slow and a surface film may form, providing that the dissolution kinetics is slower than the

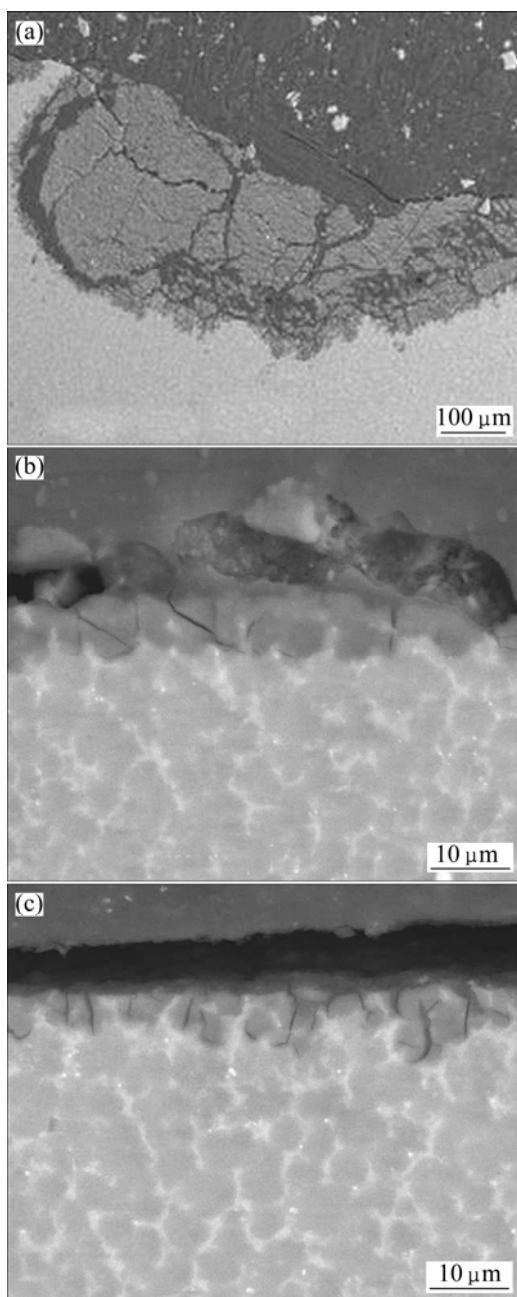


Fig.10 SEM images of cross-sections of specimens after immersion for 480 h in Na₂SO₄ solutions with different pH values: (a) pH 2; (b) pH 7; (c) pH 12

formation kinetics[11]. There was significant alkalisation near the magnesium surface in an acidic medium, and this alkalisation was associated with the formation of the surface film. The film could impede the reaction, decreasing the reaction rate. When the pH was higher than 12, the electrode potentials of H and O were more negative than those in acidic solutions. The potential of Mg began to rise, and the corrosion rate declined. As the reaction proceeded, a passive film formed on the surface as a result of the passive precipitation of Mg in alkaline solutions[12].

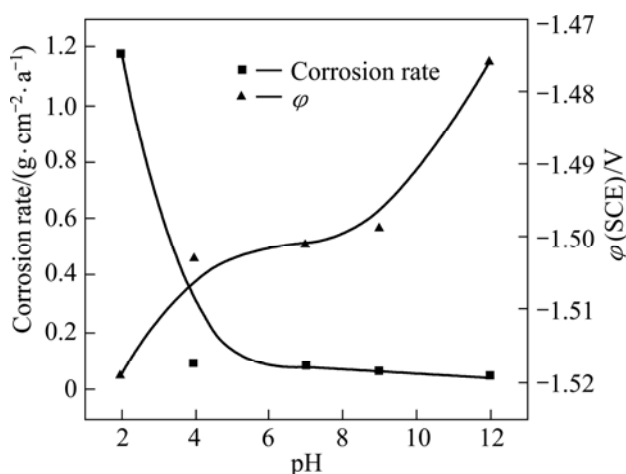
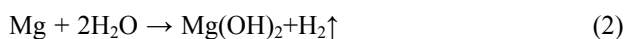


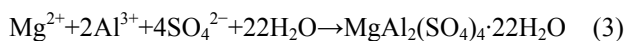
Fig.11 Electrode potential and corrosion rate of AZ91D Mg alloy in relation to pH value in Na₂SO₄ solution

4.2 Effect of pH values on corrosion behaviour of Mg alloy

The following corrosion electrochemical reaction takes place in neutral Na₂SO₄ solutions[13]:



According to YANG et al[6], the Mg(OH)₂ film is supposed to form spontaneously. Once the immersion time exceeded 6 h, the concentration of MgAl₂(SO₄)₄·22H₂O became supersaturated in the solutions. Then, MgAl₂(SO₄)₄·22H₂O began to precipitate on the surface of the specimens and became comparatively stable. The precipitation of MgAl₂(SO₄)₄·22H₂O occurred as



Pitting occurred in specimens immersed in acidic Na₂SO₄ solutions. According to CHEN et al[8], reaction (3) occurred mainly in the pitting area, while reaction (2) appeared in other areas where the film product film also formed. Furthermore, the reaction rate of reaction (3) is much higher than that of reaction (2) in the depth direction. The pitting phenomenon is shown clearly in Fig.9(a).

4.3 Corrosion surface topography

The morphologies of the corrosion products were significantly influenced by pH. In acidic solutions, general corrosion occurred from the beginning of immersion, and the corrosion products were prone to fall off as the immersion time was prolonged. This may be due to changes in the volume of the films compared with that of the matrix. Changes in the volume bring about stress between the interface of the film and the matrix[14].

In the alkaline solutions[15], the surface of Mg(OH)₂ crystals with positive charges adsorbs OH⁻ ions, which promotes the growth of Mg(OH)₂ along the borders of the specimens. Thus, the generated Mg(OH)₂ was flaky or needle-like in nature. A temperature of 20 °C is critical for the morphology of Mg(OH)₂ in weak alkaline conditions[16]. When the temperature was higher than 20 °C, Mg(OH)₂ completely transformed into flakes. This may be due to the equal rate of crystal growth in various lattice planes at higher temperatures (above 20 °C). When the temperature was less than 20 °C, the configuration of Mg(OH)₂ was needle-like. When the temperatures of the immersion tests were below 20 °C, the products formed showed a morphology shown in Fig.8(b).

Pitting is a typical form of corrosion that can occur on the surface of die-cast AZ91D Mg alloy specimens when they are immersed either in Na₂SO₄ or NaCl solution. Both sulphate and chloride ions have good nucleophilicity and are easily adsorbed on the film[17], but have different pitting initiation time. As for the specimen in NaCl solution, localized corrosion may be viewed as the outcome of a competitive process between the inhibiting properties of hydroxyl ions and the breakdown-inducing effect of chloride ions[18–19]. Chloride ions are prone to drilling through the film and inducing pitting corrosion at microstructural defect sites because of their smaller radius[20–21]. The volume of a sulphate ion is much larger than that of a chloride ion, and MgAl₂(SO₄)₄·22H₂O, as the corrosion product, is semi-permeable. Both the volume and the semi-permeable property decreased the penetration of sulphate ion. As a result, the concentration of sulphate ions that drill through the film and connect with the surface of matrix is limited. The pitting corrosion initiation time has a relationship with the ion concentration[19]. With longer immersion time, sulphate ions can traverse the protective film and finally reach the surface of the metal, allowing it to obtain its critical concentration threshold and the pitting process to begin.

5 Conclusions

1) The order of corrosion rates of Mg alloy in combination with the polarisation curves in Na₂SO₄ solutions is acidic solutions>neutral solutions>alkaline solutions. In the immersion tests, the corrosion rate of the solution with pH 2 decreases sharply until the immersion time reaches 48 h. In alkaline solutions, the corrosion rate declines slowly. In acidic or neutral solutions, the mass loss of the specimens increases sharply when the immersion time exceeds 180 h. Lower pH value induces a faster increase in mass loss. In alkaline solutions, the mass loss increases slowly and then reaches a stable level.

2) In 0.1 mol/L Na₂SO₄ solutions with various pH values, the corrosion products of the die-cast Mg alloy are mainly Mg(OH)₂ and MgAl₂(SO₄)₄·22H₂O. The morphologies of the corrosion product films change as the immersion time increases. Hemisphere-like films form on the surface of specimens in acidic solutions. In alkaline solutions, the morphology of the products changes from white reticulated lines to an acicular film and then finally to a flocculation film. In acidic solutions, pitting occurs on the surface of the specimens. Chloride ions and sulphate ions have different pitting initiation time.

References

- [1] ZENG Rong-chang, ZHANG Jin, HUANG Wei-jiu, DIETZEL W, KAINER K U, BLAWERT C, WEI K E. Review of studies on corrosion of magnesium alloys [J]. Transaction of Nonferrous Metals Society of China, 2006, 16: 763–771.
- [2] WEI Ying-hui, YANG Li-jing, HOU Li-feng, GUO Yao-wen, XU Bing-she. Formation process of bright spots on surfaces of die-cast magnesium alloy components after chemical conversion treatment [J]. Engineering Failure Analysis, 2009, 16(1): 19–25.
- [3] SONG G, ATRENS A, STJOHN D, NAIRN J, LI Y. The electrochemical corrosion of pure magnesium in 1 N NaCl [J]. Corrosion Science, 1997, 39(5): 855–875.
- [4] ZHANG Li-jun, ZHU Xu-bei, ZHANG Zhao, ZHANG Jian-qing. Electrochemical noise characteristics in corrosion process of AZ91D magnesium alloy in neutral chloride solution [J]. Transactions of Nonferrous Metals Society of China, 2009, 19(2): 496–503.
- [5] CHENG Ying-liang, QIN Ting-wei, WANG Hui-min, ZHANG Zhao. Comparison of corrosion behaviors of AZ31, AZ91, AM60 and ZK60 magnesium alloys [J]. Transactions of Nonferrous Metals Society of China, 2009, 19(3): 517–524.
- [6] YANG Li-jing, WEI Ying-hui, HOU Li-feng, ZHANG Di. Corrosion behaviour of die-cast AZ91D magnesium alloy in aqueous sulphate solutions [J]. Corrosion Science, 2010, 52(2): 345–351.
- [7] ZHANG Han-ru. The corrosion behavior of AZ91 Mg alloy in solutions [D]. Lanzhou: Lanzhou University of Technology, 2004: 21–52. (in Chinese)
- [8] CHEN Jian, WANG Jian-qiu, HAN En-hou, DONG Jun-hua, KE Wei. AC impedance spectroscopy study of the corrosion behavior of an AZ91 magnesium alloy in 0.1 mol/L sodium sulfate solution [J]. Electrochimica Acta, 2007, 52(9): 3299–3309.
- [9] CHEN Jian, WANG Jian-qiu, HAN En-hou, KE Wei. Effect of hydrogen on stress corrosion cracking of magnesium alloy in 0.1 mol/L Na₂SO₄ solution [J]. Materials Science and Engineering A, 2008, 488(1–2): 428–434.
- [10] KELLY R G, SCULLY J R, SHOESMITH D W, BUCHHEIT R G. Electrochemical techniques in corrosion science and engineering [M]. New York: Marcel Dekker, 2003: 21.
- [11] ZHAO Ming-chun, LIU Ming, SONG Guang-ling, ATRENS A. Influence of pH and chloride ion concentration on the corrosion of Mg alloy ZE41 [J]. Corrosion Science, 2008, 50(11): 3168–3178.
- [12] GAO Li-li, ZHANG Chun-hong, ZHANG Mi-lin, HUANG Xiao-mei, SHENG Nan. The corrosion of a novel Mg-11Li-3Al-0.5RE alloy in alkaline NaCl solution [J]. Journal of Alloys and Compounds, 2009, 468(1–2): 285–289.
- [13] LOPEZ-BUISAN NATTA M G. Evidence of two anodic processes in the polarization curves of magnesium in aqueous media [J]. Corrosion, 2001, 57: 712–720.
- [14] GUO Jia, YANG Shan-wu, SHANG Cheng-jia, WANG Ying, HE Xin-lai. Influence of carbon content and microstructure on corrosion behaviour of low alloy steels in a Cl⁻-containing environment [J]. Corrosion Science, 2009, 51(2): 242–251.
- [15] LV Xiao-tang, Hari Bala, LI Ming-gang, MA Xiao-kun, MA Shan-shan, GAO Ye, TANG Lan-qin, ZHAO Jing-zhe, GUO Yu-peng, ZHAO Xu, WANG Zi-chen. In situ synthesis of nanolamellas of hydrophobic magnesium hydroxide [J]. Colloids and Surfaces A, 2007, 296(1–3): 97–103.
- [16] LV Jian-ping, QIU Long-zhen, QU Bao-jun. Controlled growth of three morphological structures of magnesium hydroxide nanoparticles by wet precipitation method [J]. Journal of Crystal Growth, 2004, 267(3–4): 676–684.
- [17] ONO S, HABAZAKI H. Effect of sulfuric acid on pit propagation behaviour of aluminium under AC etch process [J]. Corrosion Science, 2009, 51(10): 2364–2370.
- [18] ABD EL HALEEM S M, ABD EL WANEES S, ABD EL AAL E E, DIAB A. Environmental factors affecting the corrosion behavior of reinforcing steel II. Role of some anions in the initiation and inhibition of pitting corrosion of steel in Ca(OH)₂ solutions [J]. Corrosion Science, 2010, 52(2): 292–302.
- [19] LI L F, SAGUES A A. Metallurgical effects on chloride ion corrosion threshold of steel in concrete [R]. Florida: University of South Florida, 2001.
- [20] SINGH S, BASU S, POSWAL A K, TOKAS R B, GHOSH S K. Electrochemically controlled pitting corrosion in Ni film: A study of AFM and neutron reflectometry [J]. Corrosion Science, 2009, 51(3): 575–580.
- [21] WANG Lei, SHINOHARA T, ZHANG Bo-Ping. Influence of chloride, sulfate and bicarbonate anions on the corrosion behavior of AZ31 magnesium alloy [J]. Journal of Alloys and Compounds, 2010, 496(1–2): 500–507.

压铸 AZ91D 镁合金在不同 pH 值的 Na_2SO_4 溶液中的腐蚀行为

田 贇¹, 杨丽景¹, 李艳芳¹, 卫英慧¹, 侯利锋¹, 李永刚¹, Ri-Ichi MURAKAMI²

1. 太原理工大学 材料科学与工程学院, 太原 030024;

2. Department of Mechanical Engineering, University of Tokushima, Tokushima 770-8506, Japan

摘 要: 研究压铸 AZ91D 镁合金在不同 pH 值的 0.1 mol/L Na_2SO_4 溶液中的腐蚀行为, 利用 SEM、FTIR 及 XRD 等手段对压铸 AZ91D 镁合金在 Na_2SO_4 溶液中的腐蚀速率、腐蚀产物形貌和腐蚀产物组分进行定量和定性分析。结果表明: 压铸 AZ91D 镁合金在不同 pH 值 Na_2SO_4 溶液中的腐蚀速率顺序从高到低依次为 pH 2, pH 4, pH 7, pH 9, pH 12, 酸性溶液的腐蚀速率大于碱性溶液的腐蚀速率; 在 Na_2SO_4 溶液中, 腐蚀产物主要为 $\text{Mg}(\text{OH})_2$ 和 $\text{MgAl}_2(\text{SO}_4)_4 \cdot 22\text{H}_2\text{O}$, 不同的 pH 值能改变腐蚀速率和腐蚀产物形貌; 氯离子和硫酸根离子有不同的点蚀引发时间。
关键词: 镁合金; 腐蚀; 硫酸钠; pH 值

(Edited by LI Xiang-qun)